JACS
JOURNAL OF THE AMERICAN CHEMICAL SOCIETY
Communication
Cite This: J. Am. Chem. Soc. 2018, 140, 4774−4777
pubs.acs.org/JACS

Investigating the Dynamics of Destabilized Nucleosomes Using Methyl-TROSY NMR

Julianne L. Kitevski-LeBlanc,*[,†] Tairan Yuwen,[†] Pamela N. Dyer,[‡] Johannes Rudolph,[‡] Karolin Luger,[‡,§] and Lewis E. Kay*[,†,∥]

[†]Departments of Chemistry, Molecular Genetics, and Biochemistry, University of Toronto, Toronto, Ontario M5S 1A8, Canada
[‡]Department of Chemistry and Biochemistry, University of Colorado, Boulder, Colorado 80309, United States
[§]Howard Hughes Medical Institute, and [∥]Program in Molecular Medicine, Hospital for Sick Children, 555 University Avenue, Toronto, Ontario M5G 1X8, Canada

Supporting Information

ABSTRACT: The nucleosome core particle (NCP), comprised of histone proteins wrapped with ∼146 base pairs of DNA, provides both protection and controlled access to DNA so as to regulate vital cellular processes. High-resolution structures of nucleosomes and nucleosome complexes have afforded a clear understanding of the structural role of NCPs, but a detailed description of the dynamical properties that facilitate DNA-templated processes is only beginning to emerge. Using methyl-TROSY NMR approaches we evaluate the effect of point mutations designed to perturb key histone interfaces that become destabilized during nucleosome remodeling in an effort to probe NCP plasticity. Notably the NCP retains its overall structural integrity, yet relaxation experiments of mutant nucleosomes reveal significant dynamics within a central histone interface associated with alternative NCP conformations populated to as much as 15% under low salt conditions. This work highlights the inherent plasticity of NCPs and establishes methyl-TROSY NMR as a valuable compliment to current single molecule methods in quantifying NCP dynamic properties.

The nucleosome is a protein−DNA complex constituting the basic unit of structural organization in the hierarchical compaction of our genome. The protein component of the nucleosome core particle consists of histone proteins H2A, H2B, H3, and H4 which form an octamer through the assembly of two H2A−H2B heterodimers and one H3−H4 tetramer.[1] The octamer acts as a spool around which ∼146 base pairs of DNA are wrapped with linker sequences connecting neighboring NCPs to form the familiar "beads on a string" model found in active euchromatic genomic regions.[1,2] NCPs present a steric barrier restricting DNA access to proteins and enzymes essential for fundamental processes such as replication, transcription, and repair.[3−5] Recent studies have shown that NCPs are more dynamic than previously assumed, and although the canonical NCP structure observed in numerous crystal structures appears to be the most populated conformation, alternative excited states, in both the presence and absence of external factors, do exist and are functionally relevant.[6−10]

Herein we examine the inherent plasticity of the NCP by evaluating the effect of a series of destabilizing mutants on nucleosome structure and dynamics. Mutants were designed to weaken the histone dimer−tetramer interface due to its integral role in overall NCP stability and in DNA-templated processes, where dimer loss has been shown experimentally or implicated.[11] The effects of these mutations are examined using methyl-TROSY NMR experiments that provide enhanced sensitivity and spectral resolution for large macromolecules.[12] In such experiments protonated methyl groups, in an otherwise deuterated environment, provide powerful reporters of structure and dynamics in proteins and protein complexes up to ∼1 MDa.[13−15] Destabilization of the octamer was achieved through point mutations of key residues in histone H4 (H4Y98) and histone H3 (H3A98) (Figure 1A), which are sandwiched between the dimer and tetramer units. We prepared NCPs with octamers bearing one of two single mutants (H4Y98H or H4Y98W) as well as a double mutant (H3A98H/H4Y98H), with the H4Y98H mutation alone sufficient to render the octamer unstable in the absence of DNA (Figure S1). The relative stabilities of the wild type (WT) and mutant NCPs were examined using a DNA competition assay that measures the concentration of competitor DNA required to disrupt the canonical NCP by abstracting one or both dimers (Figure S2). The stabilities of the mutants employed fall into the following order from highest to lowest: WT ≈ H4Y98W > H4Y98H > H3A98H/H4Y98H, pH 6 (Table S1). Notably, this decreased stability has functional effects, as nucleosomes with the H4Y98H mutation offer less resistance toward an advancing RNA polymerase in *in vitro* transcription experiments.[8]

The structural integrity of each of the mutant NCPs was evaluated by NMR using highly deuterated samples prepared with Ileδ1-[$^{13}CH_3$], Leu,Val-[$^{13}CH_3$,$^{12}CD_3$]-H2B (referred to as ILV-methyl labeled in what follows), and perdeuterated H2A, H3, and H4 to preserve spectral resolution in the 210 kDa complex. H2B was selected as the reporter histone for our studies because of its contribution to the largest dimer−tetramer interface, via a 4-helix bundle formed with H4, as well as its superior spectral quality.[17] Due to the exquisite sensitivity

Received: January 24, 2018
Published: March 28, 2018

DOI: 10.1021/jacs.8b00931
J. Am. Chem. Soc. 2018, 140, 4774−4777

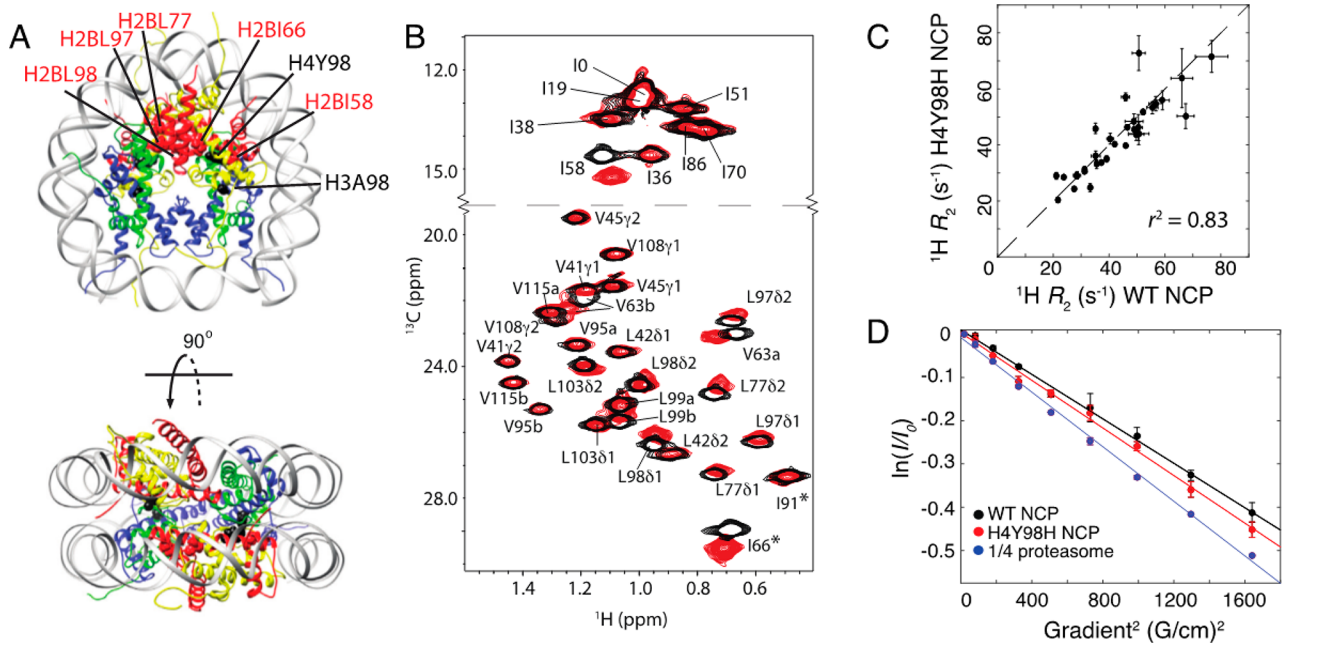

Figure 1. (A) Crystal structure of the *D. melanogaster* NCP (2PYO[16]) with location of point mutations identified in black and residues exhibiting effects due to the introduced mutations labeled in red. Color scheme: H2A, yellow; H2B, red; H3, blue; H4, green. (B) Overlay of $^{1}H-^{13}C$ HMQC spectra of ILV-methyl labeled H2B WT (black) and H4Y98H (red) NCPs collected at 18.7 Tesla (T), 45 °C with assignments indicated. In cases where stereospecific assignments are not available, prochiral methyl groups are labeled as a,b and aliased peaks are indicated with *. (C) Correlation of ^{1}H transverse relaxation rates (R_2) measured in ILV-methyl labeled H2B in WT and H4Y98H NCPs. Data sets recorded at 14.0T, 45 °C. (D) Experimental data (circles) and fits (lines) from translational diffusion measurements of ILV-methyl labeled H2B WT (black), H4Y98H NCPs (red), and 1/4 proteasome (blue), 14.0T, 25 °C (see SI).

of chemical shifts to structural perturbations, a rapid assessment of the effects of mutations on protein structure can be obtained through comparison of $^{1}H-^{13}C$ HMQC spectra of WT and mutant NCPs. Figure 1B shows an overlay of spectra of WT (black) and H4Y98H (red) ILV-methyl labeled H2B NCPs with peak assignments indicated. Methyl probes near the mutated amino acid, for example I58, V63a,b, and I66 (aliased in spectra), exhibit the largest chemical shift perturbations (CSPs), while those located within the 4-helix bundle formed between H2B and H4, for example L77δ2, L97δ2, and L98δ1/δ2, exhibit moderate changes. The magnitude and direction of CSPs were similar for H4Y98W and H3A98H/H4Y98H NCPs (Figure S3). Overall the spectra overlay very well, indicating that the conformation of H2B is similar in WT and all mutant NCPs employed. We have measured ^{1}H transverse relaxation rates of the slowly relaxing ^{1}H single-quantum methyl transitions[18] (R_2) to evaluate the dynamics of methyl probes on the ps−ns time scale. Figure 1C shows a good correlation between R_2 values measured in WT and H4Y98H ILV-methyl labeled H2B NCPs, indicating that fast time scale dynamics are similar for most H2B methyl groups. Finally, to confirm that the H4Y98H mutant NCP maintains the full complement of histones and is an intact particle under our NMR conditions, we measured translational diffusion coefficients, D, of WT and H4Y98H NCPs as well as of a 180 kDa single ring construct of the proteasome (1/4 proteasome[19]) using ^{13}C-edited diffusion NMR experiments. The values obtained, $D = (3.6 \pm 0.1) \times 10^{-7}$ cm^2/s and $(3.8 \pm 0.2) \times 10^{-7}$ cm^2/s (25 °C) for the WT and H4Y98H NCPs, respectively, are the same within experimental error and are similar to that of the 1/4 proteasome, where a value of $D = (4.5 \pm 0.1) \times 10^{-7}$ cm^2/s was measured under identical conditions.

Methyl-TROSY CPMG relaxation dispersion experiments[20] monitor μs−ms time scale motions and have been instrumental for understanding the functional role of dynamics in a host of macromolecular machines.[21−23] Here the effective transverse relaxation rate ($R_{2,\mathrm{eff}}$) is measured as a function of refocusing pulse frequencies (ν_{CPMG}), which serve to quench the effects of conformational exchange, producing so-called dispersion profiles.[24] Such profiles can be fit to extract the rate of exchange between interconverting ground and excited (often invisible) conformational states, k_{ex}, the population of the excited state, p_E, and the chemical shift differences between the corresponding spins in the exchanging states, $|\Delta\varpi|$ (ppm). Here we employed methyl-TROSY CPMG experiments to establish whether destabilization of NCPs by mutation leads to the formation of alternate conformational states and, if so, whether their relative populations scale with NCP stability. Figure 2A shows profiles (18.7T, 45 °C) obtained for six methyl probes that were found to exhibit measurable dispersions in H4Y98H and H3A98H/H4Y98H NCPs. In contrast, flat profiles were measured for both WT and the H4Y98W mutant, consistent with the greater stability of these two NCPs (Table S1).

Residues with conformational exchange cluster to a region of H2B involved in a 4-helix bundle with H4, a main point of contact between the dimer and tetramer units (Figure S4). Values of $(p_E, k_{ex}) = (8.2 \pm 0.5\%, 742 \pm 30\ s^{-1})$ and $(15.6 \pm 1.4\%, 963 \pm 33\ s^{-1})$ for H4Y98H and H3A98H/H4Y98H NCPs, respectively, are obtained from global fits of 14.0 and 18.7T data sets (Figure S5). ^{13}C chemical shift differences ($|\Delta\varpi|$) obtained from global fits of the two mutants independently exhibit a high correlation (Figure 2B), indicating that the conformational exchange processes in these two samples involve the same excited state, whose population is

DOI: 10.1021/jacs.8b00931
J. Am. Chem. Soc. 2018, 140, 4774−4777

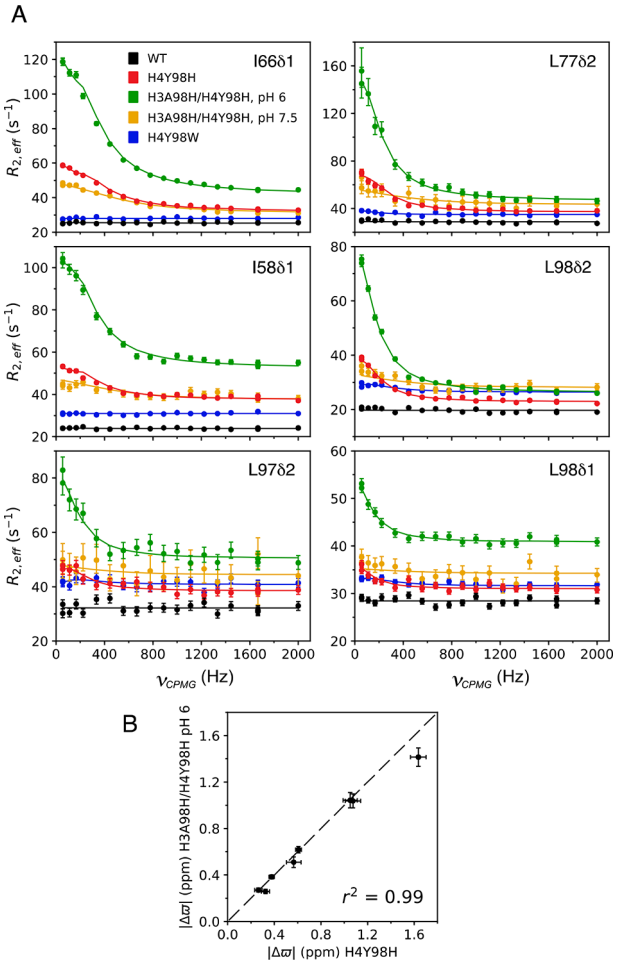

Figure 2. (A) Experimental data points (circles) and best fits (lines) for methyl-TROSY CPMG dispersions recorded on ILV-methyl labeled H2B NCPs, as indicated (18.7T (mutants), 14.0T (WT), 45 °C). (B) Correlation of extracted ^{13}C $|\Delta\varpi|$ values from separate global fits of dispersion profiles measured on ILV-methyl labeled H2B H4Y98H and H3A98H/H4Y98H pH 6 NCP samples, 14.0 and 18.7T.

nearly doubled in the H3A98H/H4Y98H mutant. The difference in ΔG values between ground and excited states in the single and double mutants, based on p_E values, is 0.4 kcal/mol. Assuming that the mutations principally effect stabilities of the ground states and, further, that the negligibly small dispersions for the WT NCP correspond to p_E < 1% (Figure S6), then the H4Y98H and H3A98H/H4Y98H mutations are calculated to destabilize the ground state by at least 1.4 and 1.8 kcal/mol, respectively (see SI). Notably, we observed a pH dependence for the dispersion profiles of the H3A98H/H4Y98H NCP, with profiles significantly reduced at pH 7.5 in comparison to pH 6 (Figure 2). Within proteins, histidine side chains have average pK_a values of 6.6 ± 1.0;[25] thus, the imidazole moiety is likely to be positively charged at pH 6 and neutral at pH 7.5. This implies that the origin of the observed destabilization in the single and double mutants is likely due to positive charges in the center of the octamer. Although our NMR studies establish the time scale of the exchange process, the relative energetics of the interconverting states, and the regions of the NCP that are most affected structurally, they do not provide a picture of the excited state. Recent cryoEM studies have revealed multiple NCP conformations promoted by asymmetric DNA unwrapping;[10] however, these are unlikely to correspond to what is observed here (see SI text).

Our studies use NCPs wrapped with highly optimized 601 DNA, a sequence that is known to form stable and homogeneous NCP samples ideal for biophysical analysis.[26,27] To evaluate the effect of an alternative DNA sequence we prepared NCPs using our most destabilized octamer containing the H3A98H/H4Y98H pair of mutations with DNA corresponding to the gene for 5S rRNA (Figure S7). While both 601 and 5S rRNA DNA sequences have been successfully used for biophysical analysis of recombinant NCPs, measures of their relative affinities for octamer revealed a net increased stabilization of 2.9 kcal/mol for 601 DNA[26] and increased positioning power, producing more homogeneous NCPs.[28] Figure 3A shows an overlay of spectra of H3A98H/H4Y98H

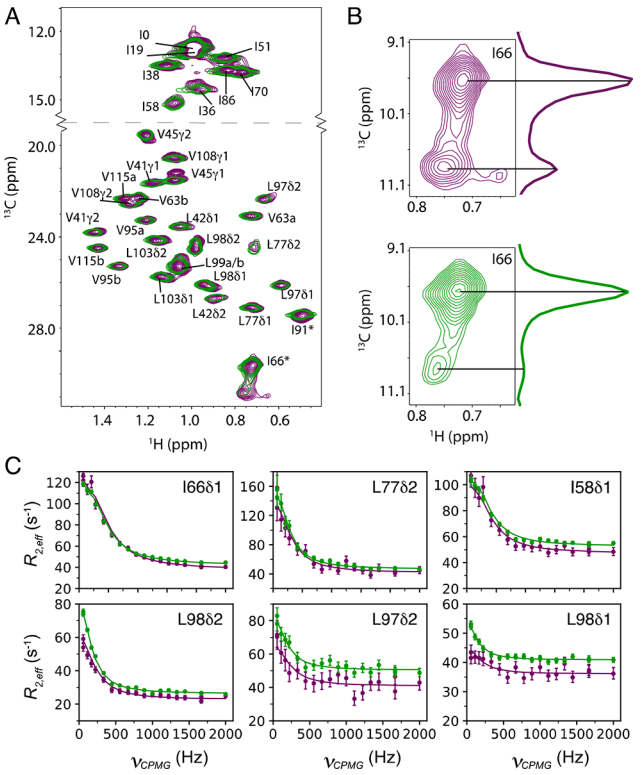

Figure 3. (A) Overlay of ^{1}H−^{13}C HMQC spectra of H3A98H/H4Y98H ILV-methyl labeled H2B NCPs wrapped with 601 (green) or 5S rRNA (purple) DNA, 18.7T, 45 °C. Aliased residues indicated with *. (B) Regions of ^{1}H−^{13}C HMQC spectra with associated 1D slices along ^{13}C dimensions highlighting major and minor peaks associated with residue I66. (C) Experimental data points (circles) and best fits (lines) for methyl-TROSY CPMG dispersion profiles recorded on NCP samples indicated in A (18.7T, 45 °C).

ILV-methyl labeled H2B octamers wrapped with 601 (green) or 5S rRNA DNA (purple). Similar to comparisons between WT and mutant NCPs, the ^{1}H−^{13}C HMQC spectra overlay well, indicating that the ground state conformations for NCPs prepared with both types of DNA are similar. Careful inspection of the I66 correlation at low contour levels reveals a minor peak that is significantly larger for the 5S rRNA NCP relative to the NCP generated with 601 DNA (ratio of minor/major peak volumes ∼5 times larger). CPMG dispersion profiles for NCPs prepared with 601 and 5S rRNA DNA are very similar (Figure 3C), with comparable extracted exchange rates, populations, and a high correlation among $|\Delta\varpi|$ values

DOI: 10.1021/jacs.8b00931
J. Am. Chem. Soc. 2018, 140, 4774−4777

(Figure S8). The value of p_E obtained from analysis of CPMG data recorded on the double mutant with 5S rRNA DNA (16 ± 4%) is distinct from that calculated based on the ratio of major/minor cross-peak volumes for I66 (~35%), suggesting that the observable minor peak has a different origin than the excited conformation characterized by relaxation dispersion. In this study we have introduced a series of perturbations within the octameric NCP core, focusing on a particularly important region for chromosome remodeling. Notably, the ground state structures of the resulting NCPs are robust to the changes introduced, yet the mutations do result in significant populations of excited conformational states that lead to increased *in vitro* transcription rates,[8] while the innate flexibility of the NCP can facilitate nucleosome repositioning in the presence of a remodeler.[9] In the course of normal cellular activities nucleosomes must tolerate numerous perturbations including substitution of canonical histones for variants, post-translational modifications, and the action of histone chaperones and chromatin remodelers. The inherent NCP plasticity, as established here, is likely a key property in facilitating its opposing roles as both a structural scaffold in genome compaction and a functional participant in DNA-templated processes.

■ ASSOCIATED CONTENT

Supporting Information

The Supporting Information is available free of charge on the ACS Publications website at DOI: 10.1021/jacs.8b00931.

Materials and Methods, Figures S1−S8, and Table S1 (PDF)

■ AUTHOR INFORMATION

Corresponding Authors

*kay@pound.med.utoronto.ca

*jkitevski@gmail.com

ORCID

Tairan Yuwen: 0000-0003-3504-7995

Lewis E. Kay: 0000-0002-4054-4083

Notes

The authors declare no competing financial interest.

■ ACKNOWLEDGMENTS

This research was supported by grants from the Canadian Institutes of Health Research (L.E.K.) and the Howard Hughes Medical Institute (K.L.). L.E.K. holds a Canada Research Chair in Biochemistry.

■ REFERENCES

(1) Luger, K.; Mäder, A. W.; Richmond, R. K.; Sargent, D. F.; Richmond, T. J. *Nature* **1997**, *389*, 251.

(2) McGinty, R. K.; Tan, S. *Chem. Rev.* **2015**, *115*, 2255.

(3) Price, B. D.; D'Andrea, A. D. *Cell* **2013**, *152*, 1344.

(4) Gaykalova, D. A.; Kulaeva, O. I.; Volokh, O.; Shaytan, A. K.; Hsieh, F. K.; Kirpichnikov, M. P.; Sokolova, O. S.; Studitsky, V. M. *Proc. Natl. Acad. Sci. U. S. A.* **2015**, *112*, E5787.

(5) Chang, H. W.; Pandey, M.; Kulaeva, O. I.; Patel, S. S.; Studitsky, V. M. *Sci. Adv.* **2016**, *2*, e1601865.

(6) Bohm, V.; Hieb, A. R.; Andrews, A. J.; Gansen, A.; Rocker, A.; Toth, K.; Luger, K.; Langowski, J. *Nucleic Acids Res.* **2011**, *39*, 3093.

(7) Winkler, D. D.; Luger, K. *J. Biol. Chem.* **2011**, *286*, 18369.

(8) Hsieh, F. K.; Kulaeva, O. I.; Patel, S. S.; Dyer, P. N.; Luger, K.; Reinberg, D.; Studitsky, V. M. *Proc. Natl. Acad. Sci. U. S. A.* **2013**, *110*, 7654.

(9) Sinha, K. K.; Gross, J. D.; Narlikar, G. J. *Science* **2017**, *355*, eaaa3761.

(10) Bilokapic, S.; Strauss, M.; Halic, M. *Nat. Struct. Mol. Biol.* **2018**, *25*, 101.

(11) Lai, W. K. M.; Pugh, B. F. *Nat. Rev. Mol. Cell Biol.* **2017**, *18*, 548.

(12) Tugarinov, V.; Hwang, P. M.; Ollerenshaw, J. E.; Kay, L. E. *J. Am. Chem. Soc.* **2003**, *125*, 10420.

(13) Sprangers, R.; Kay, L. E. *Nature* **2007**, *445*, 618.

(14) Rosenzweig, R.; Kay, L. E. *Annu. Rev. Biochem.* **2014**, *83*, 291.

(15) Gelis, I.; Bonvin, A. M.; Keramisanou, D.; Koukaki, M.; Gouridis, G.; Karamanou, S.; Economou, A.; Kalodimos, C. G. *Cell* **2007**, *131*, 756.

(16) Clapier, C. R.; Chakravarthy, S.; Petosa, C.; Fernandez-Tornero, C.; Luger, K.; Muller, C. W. *Proteins: Struct., Funct., Genet.* **2008**, *71*, 1.

(17) Kato, H.; van Ingen, H.; Zhou, B. R.; Feng, H. Q.; Bustin, M.; Kay, L. E.; Bai, Y. W. *Proc. Natl. Acad. Sci. U. S. A.* **2011**, *108*, 12283.

(18) Tugarinov, V.; Kay, L. E. *J. Am. Chem. Soc.* **2006**, *128*, 7299.

(19) Religa, T. L.; Sprangers, R.; Kay, L. E. *Science* **2010**, *328*, 98.

(20) Korzhnev, D. M.; Kloiber, K.; Kanelis, V.; Tugarinov, V.; Kay, L. E. *J. Am. Chem. Soc.* **2004**, *126*, 3964.

(21) Sprangers, R.; Gribun, A.; Hwang, P. M.; Houry, W. A.; Kay, L. E. *Proc. Natl. Acad. Sci. U. S. A.* **2005**, *102*, 16678.

(22) Schutz, A. K.; Rennella, E.; Kay, L. E. *Proc. Natl. Acad. Sci. U. S. A.* **2017**, *114*, E6822.

(23) Traaseth, N. J.; Veglia, G. *Biochim. Biophys. Acta, Biomembr.* **2010**, *1798*, 77.

(24) Palmer, A. G., 3rd; Grey, M. J.; Wang, C. *Methods Enzymol.* **2005**, *394*, 430.

(25) Grimsley, G. R.; Scholtz, J. M.; Pace, C. N. *Protein Sci.* **2009**, *18*, 247.

(26) Lowary, P. T.; Widom, J. *J. Mol. Biol.* **1998**, *276*, 19.

(27) Thastrom, A.; Lowary, P. T.; Widlund, H. R.; Cao, H.; Kubista, M.; Widom, J. *J. Mol. Biol.* **1999**, *288*, 213.

(28) Dyer, P. N.; Edayathumangalam, R. S.; White, C. L.; Bao, Y.; Chakravarthy, S.; Muthurajan, U. M.; Luger, K. *Methods Enzymol.* **2003**, *375*, 23.

DOI: 10.1021/jacs.8b00931
J. Am. Chem. Soc. 2018, 140, 4774−4777